

## OR2-1

小型超音速飛行実験機向け推進供給システムに関する研究  
(イソプロパノールを用いた推進捕捉機構の性能検証)

## Study on Propellant Supply System for Small-scale Supersonic Flight Experiment Vehicle (Evaluation of the Propellant Management Device Using Isopropanol)

○穴田 蒼輝<sup>1</sup>, 今井 良二<sup>1</sup>, 湊 亮二郎<sup>1</sup>, 中田 大将<sup>2</sup>, 内海 政春<sup>2</sup>

○Aoki ANADA<sup>1</sup>, Ryoji IMAI<sup>1</sup>, Ryojiro MINATO<sup>1</sup>, Daisuke NAKATA<sup>2</sup>, Masaharu UCHIUMI<sup>2</sup>

<sup>1</sup>室蘭工業大学, Muroran Institute of Technology

<sup>2</sup>室蘭工業大学, 航空宇宙機システム研究センター, APReC, Muroran Institute of Technology

### 1. Introduction

The Aerospace Plane Research Center in Muroran Institute of Technology is developing the small-scale supersonic flight experiment vehicle as a flying test bed for a technical demonstration in high-speed flight environment. In the small-scale supersonic flight experiment vehicle, the liquid supplying system for Bioethanol and liquid oxygen (LOX) by nitrogen pressurant has been studied. However, sloshing is expected to occur in this liquid fuel tank by the acceleration during flight. It is feared that the risk of adverse effects on the attitude control of the aircraft and the propulsion system by the inclusion of pressurized gas in the supplied fuel increase due to sloshing.

The purpose of this paper is to research and develop a propellant management device (PMD) which suppresses gas entrainment in the aircraft fuel tank and evaluate its performance.

### 2. Theory

**Figure 1** shows a structure of the PMD. The PMD is installed on the reservoir outlet. A commonly used the PMD utilizes metal wire screen meshes. The porous screen uses capillary forces to reject vapor bubbles trying to penetrate the screen, as shown in **Fig. 1**, while allowing only liquid to flow through. The bubble point pressure ( $\Delta P_{BP}$ ) is defined as pressure across the porous screen that causes vapor bubbles to pass through the porous screen and reach the liquid side <sup>1)</sup>. The equation used for  $\Delta P_{BP}$  is given in Eq. (1):

$$\Delta P_{BP} = \frac{4\gamma \cos \theta}{D_p}, \quad (1)$$

where  $\gamma$  is the surface tension of the liquid,  $\theta$  is the contact angle of the liquid on the screen, and  $D_p$  is the pore diameter of the screen. As shown in Eq. (2), vapor bubbles to pass through the porous screen, if the static pressure difference between the vapor and liquid phases at the porous screen is less than  $\Delta P_{BP}$ :

$$\Delta P_{BP} > P_V - P_L, \quad (2)$$

where  $P_V$  is the static pressure of the vapor phase, and  $P_L$  is the static pressure of the liquid phase.  $P_V - P_L$  is equal to the total pressure drop ( $\Delta P_{total}$ ) across the PMD system:

$$P_V - P_L = \Delta P_{total} \quad (3)$$

$\Delta P_{total}$  can be expressed as a sum of the constituent parts:

$$\Delta P_{total} = \Delta P_{FTS} + \Delta P_{friction}, \quad (4)$$

where  $\Delta P_{FTS}$  is the flow-through-screen pressure drop due to liquid flow across the porous screen, and  $\Delta P_{friction}$  is the frictional loss down the PMD. From Eqs. (2) and (3), if  $\Delta P_{total}$  of the PMD system does not exceed  $\Delta P_{BP}$ , the vapor bubbles cannot pass through the porous screen:

$$\Delta P_{BP} > \Delta P_{total}, \quad (5)$$

Eq. (5) indicates that the vapor flow during the transfer process can be shut off if  $\Delta P_{total}$  in the PMD does not exceed  $\Delta P_{BP}$ .

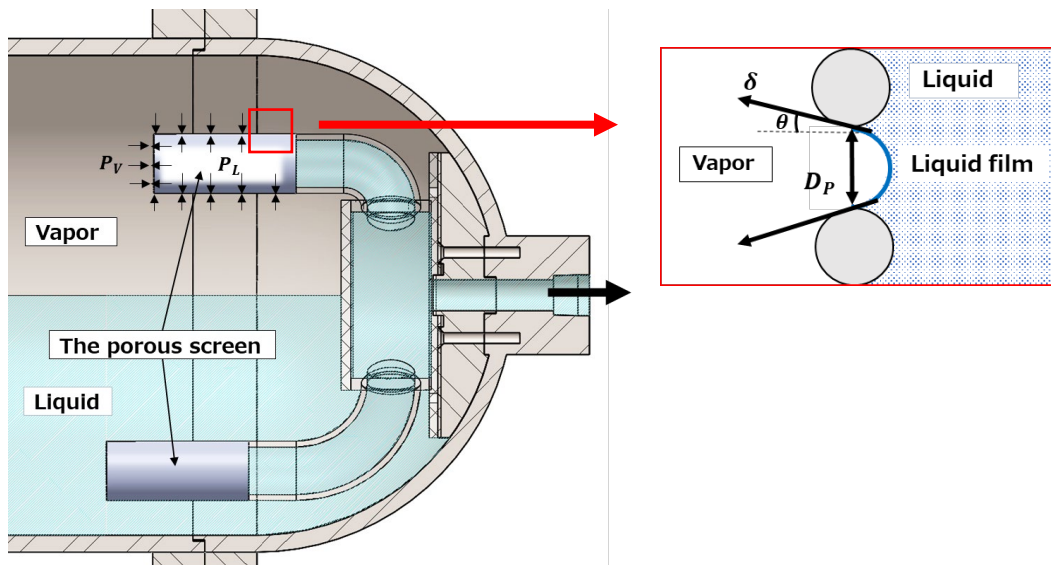


Figure 1. Installation of the PMD.

### 3. Optimization of the PMD geometry

In order to decide the PMD geometry satisfying the required performance of the flight model, the computational fluid dynamics (CFD) simulation of isopropanol (IPA) passing through the PMD is conducted.

#### 3.1. Bubble point pressure

In this research, we adopt the porous screen called the 325 × 2300 Dutch Twill screen, which is generally used to study on the PMD using IPA.

In general,  $\gamma$  is known to be a function of temperature and is well represented by <sup>2)</sup>:

$$\gamma = \gamma_0 \left( 1 - \frac{T}{T_c} \right)^{a_0 - a_1 \frac{T}{T_c} + a_2 \left( \frac{T}{T_c} \right)^2}, \quad (6)$$

where  $T$  is the temperature of the liquid at the PMD,  $T_c$  is the critical temperature, and  $\gamma_0$ ,  $a_0$ ,  $a_1$ ,  $a_2$ , are fitting parameters. When IPA is used,  $T = 298.15$  K,  $T_c = 508.3$  K,  $\gamma_0 = 46.507$  mN/m,  $a_0 = 0.901$ ,  $a_1 = 0$ , and  $a_2 = 0$ . From above,  $\gamma$  can be found as 20.993 mN/m.

When IPA is used,  $\theta$  is  $6.3^\circ$ .

$D_p$  of the  $325 \times 2300$  Dutch Twill screen is  $14.47 \mu\text{m}$  <sup>1)</sup>.

As a result of substituting each calculated variable into Eq. (1),  $\Delta P_{BP}$  becomes 6400 Pa.

### 3.2. The CFD simulation of IPA passing through the PMD from the reservoir

#### 3.2.1. The CFD model

In this research, we use the commercial CFD code ANSYS FLUENT 2021 R1. the CFD simulation reveals  $\Delta P_{total}$  in the PMD and the length of the porous cylindrical screen attached to tip of nozzles,  $L$  shown in **Fig. 2**. The PMD has 4 nozzles. IPA passes through these nozzles and flows outward. They have an inner diameter of 20 mm. **Figure 3** shows the assembly model of the reservoir and the PMD. The diameter of this reservoir is 202 mm and its overall length is 456 mm. **Figure 4** shows the computational model of it. Since the assembly model has mirror symmetry, the extent of the computational model can be reduced to half of the overall assembly model, as shown in **Fig. 4**. This computational model assumes flow when the liquid level drops to the center of the reservoir.

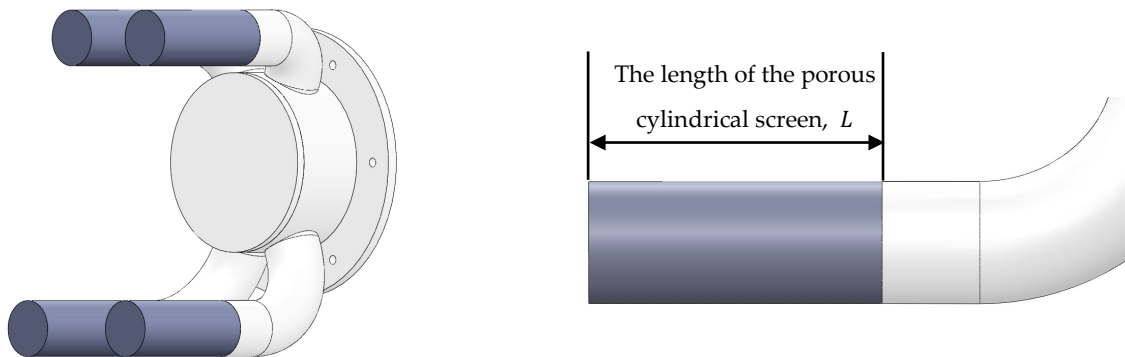


**Figure 2.** The geometry of the PMD.

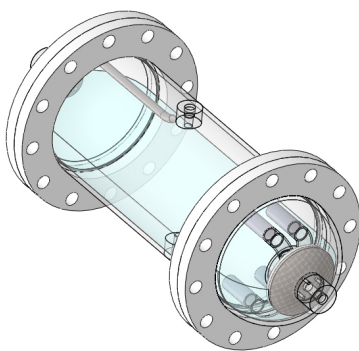


**Figure 3.** The assembly model of the reservoir and the PMD.

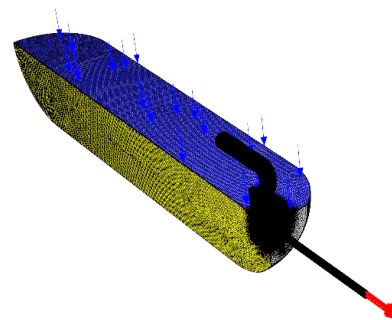


**Figure 4.** The computational model.

The equation used for  $\Delta P_{FTS}$  is given in Eq. (7) <sup>3)</sup>:

$$\Delta P_{FTS} = A \left( \frac{Q\delta\mu a^2}{\varepsilon^2} \right) U + B \left( \frac{Q\delta\rho}{\varepsilon^2 D_p} \right) U^2, \quad (7)$$

where  $A$  and  $B$  is the curve fittings parameters,  $Q$  is the tortuosity factor of the porous screen,  $\delta$  is the porous screen thickness,  $a$  is the surface area to volume ratio,  $\varepsilon$  is the void fraction,  $U$  is the fluid velocity, and  $\mu$  is the viscosity, and  $\rho$  is the density of the fluid. For  $325 \times 2300$  Dutch Twill screen,  $A = 6.36$  and  $B = 1.347$ , while  $Q = 1.28$ ,  $\delta = 82.3 \mu\text{m}$ ,  $a = 0.1077 \mu\text{m}^{-1}$ ,  $\varepsilon = 0.331$ ,  $D_p = 14.47 \mu\text{m}$  <sup>1)</sup>. Since the porous screen is too thin to create the computational model, it is treated as a ‘‘porous-jump’’. In FLUENT,  $\Delta P_{FTS}$  is calculated using Eq. (8):

$$\Delta P_{FTS} = \left( \frac{\mu}{\alpha} U + C_2 \frac{1}{2} \rho U^2 \right) \Delta m, \quad (8)$$

where  $\alpha$  is the face permeability of the porous screen,  $C_2$  is the pressure-jump coefficient, and  $\Delta m$  is the thickness of the porous screen. Two major parameters for the porous jump in FLUENT,  $\alpha$  and  $C_2$ , are determined from Eqs. (7) and (8):

$$\alpha = \frac{\varepsilon}{AQa^2} = 1.16027 \times 10^{-12} \text{ m}^2, \quad (9)$$

$$C_2 = \frac{2BQ}{\varepsilon^2 D_p} = 2.17512 \times 10^6 \text{ 1/m}, \quad (10)$$

$$\Delta m = \delta = 82.3 \mu\text{m}, \quad (11)$$

**Figure 5** shows each boundary condition. The inlet condition is set pressure boundary condition of 0.3 MPa. Since the liquid level descends horizontally, the inlet boundary is set as a plane from **Fig. 5**. The outlet condition is set pressure boundary condition of atmospheric pressure and 0.234 kg/s as target mass-flow rate. This outlet boundary is in a zone of the fully developed pipe flow. Other faces are treated as walls.

From Eq. (3), to calculate  $\Delta P_{total}$ ,  $P_L$  is obtained from the CFD simulation results.  $P_L$  is static pressure of liquid on the inner wall of the upper porous screen shown in **Fig. 6**.  $P_V$  is 0.3 MPa, the same pressure set by the inlet boundary condition.

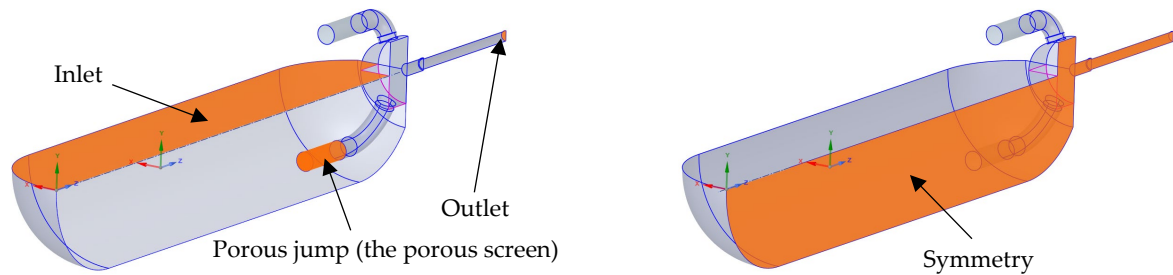


**Figure 5.** Each boundary condition in the assembly model.

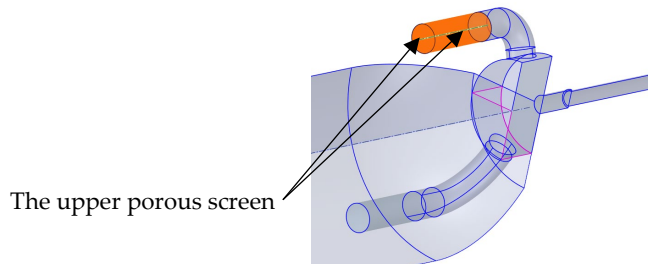


**Figure 6.** The static pressure distribution in the assembly model.

### 3.2.2. The CFD simulation results

The CFD simulation is conducted when  $L$  is 30 mm, 60 mm, 70 mm, and 80 mm. The static pressure distribution inside the PMD is shown in **Fig. 7**. By increasing the value of  $L$ , the static pressure inside the PMD increases. If the volumetric flow rate of liquid through the porous screen is constant, flow velocity and area inversely proportional. Therefore, from Eq. (7), by lengthening  $L$ , i.e., increasing surface area of the porous screen,  $\Delta P_{FTS}$  decreases and the static pressure inside the PMD increases.

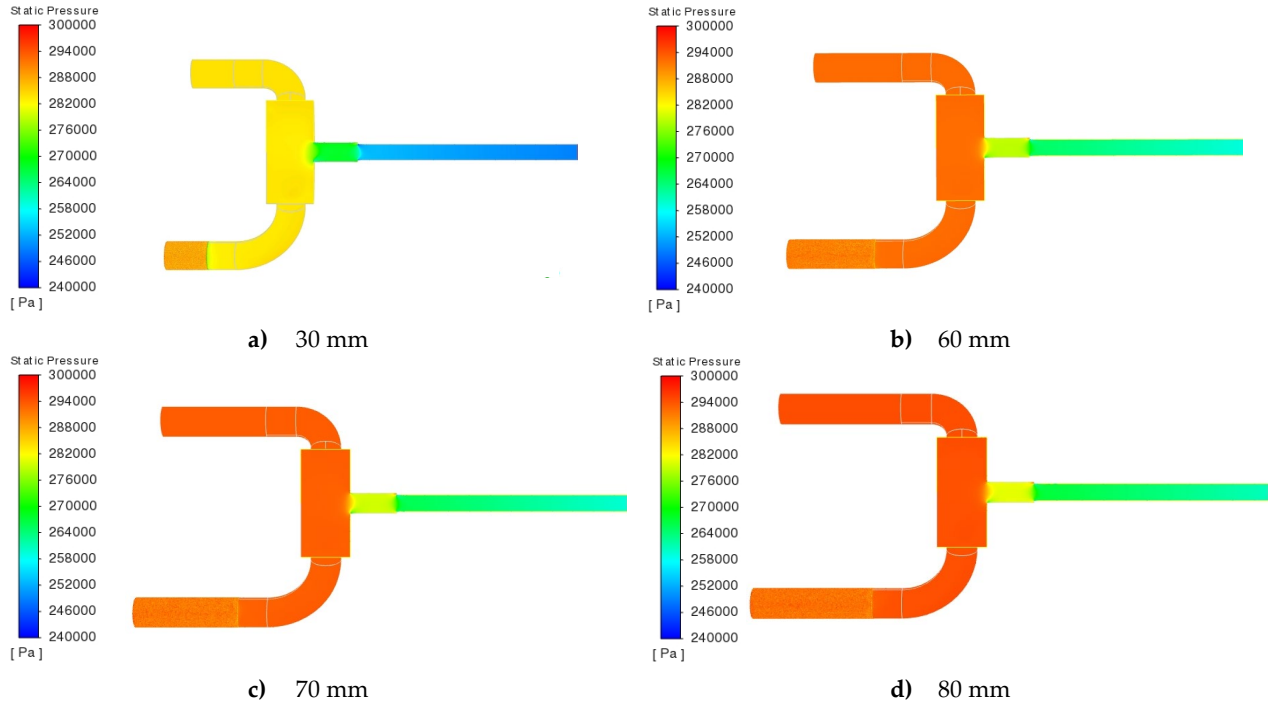


**Figure 7.** The static pressure distribution inside the PMD.

**Figure 8** shows the static pressure distribution of the assembly model when  $L$  is 80 mm. To make the static pressure distribution at the outer wall of the PMD easier to see, some areas of the symmetry boundary are hidden. **Figure 8** shows that the static pressure inside the PMD is lower than the static pressure inside the reservoir. This CFD simulation results can reproduce the pressure drop across the porous screen used in this research.

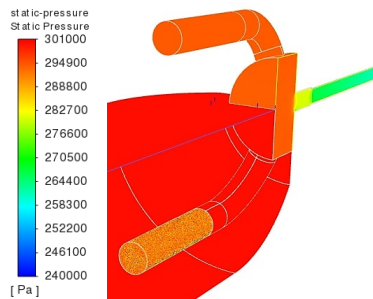


**Figure 8.** The static pressure distribution of the assembly model when  $L$  is 80 mm.

**Table 1** shows the value of  $P_L$  and  $\Delta P_{total}$  for each length of the porous cylindrical screen. Since  $\Delta P_{BP}$  of the  $325 \times 2300$  Dutch Twill screen when IPA is used is 6400 Pa, **Table 1** shows that Eq. (2) is satisfied when  $L$  is 80 mm.

**Table 1.** Static pressure distribution in the assembly model.

| The length of the porous cylindrical screen, $L$ (mm) | The static pressure of liquid phase, $P_L$ (Pa) | The total pressure drop, $\Delta P_{total}$ (Pa) |
|---|---|--|
| 30  | 282867  | 17133  |
| 60  | 292549  | 7451   |
| 70  | 293444  | 6556   |
| 80  | 294506  | 5494   |

#### 4. Future experiment schedule

We will discuss the PMD performance evaluation experiments that will be conducted in the future.

In order to evaluate performance of the PMD, the horizontal liquid outflow test using a model reservoir. **Figure 9** shows the piping diagram of this experiment. GN<sub>2</sub> is then used to pressurize the reservoir using a ball valve mounted at downstream to the reservoir until outflow is completed. The measurement items are the pressure in the reservoir, the temperature in it, and the volumetric flow rate at downstream to it. It used in the experiment is made stainless steel. As shown in **Fig. 10**, the PMD is installed at the reservoir outlet. In order to confirm that the PMD is able to suppress gas entrainment, it is necessary to visualize the inside of the PMD. Therefore, this PMD is made of polycarbonate, and the four nozzles are made of glass. We pressurize the reservoir at 0.3 MPa and confirm whether the PMD can suppress gas entrainment. The liquid used in the experiment is IPA.

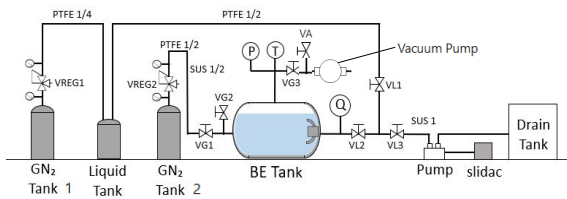


**Figure 9.** The piping diagram of the horizontal liquid outflow test.

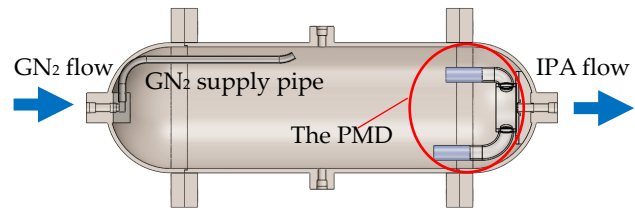


**Figure 10.** The PMD mounted to the reservoir outlet.

we also need to evaluate the performance of the PMD under condition of acceleration acting on the reservoir. Therefore, we will reproduce the inclination of the liquid level in the reservoir under acceleration and conduct the liquid outflow test using IPA.

#### References

- 1) C. F. Camarotti: Screen Database Development for the Influential Factors of Liquid Acquisition Device Screens, 2017.
- 2) J. W. Hartwig and Y. Kamotani: The Static Bubble Point Pressure Model for Cryogenic Screen Channel Liquid Acquisition Devices, International Journal of Heat and Mass Transfer, 2016.
- 3) J. Armour and J. Cannon: Fluid Flow Through Woven Screens, AIChE, vol. 14, no. 3, pp. 415, 1968.



© 2022 by the authors. Submitted for possible open access publication under the terms and conditions of the Creative Commons Attribution (CC BY) license (<http://creativecommons.org/licenses/by/4.0/>).